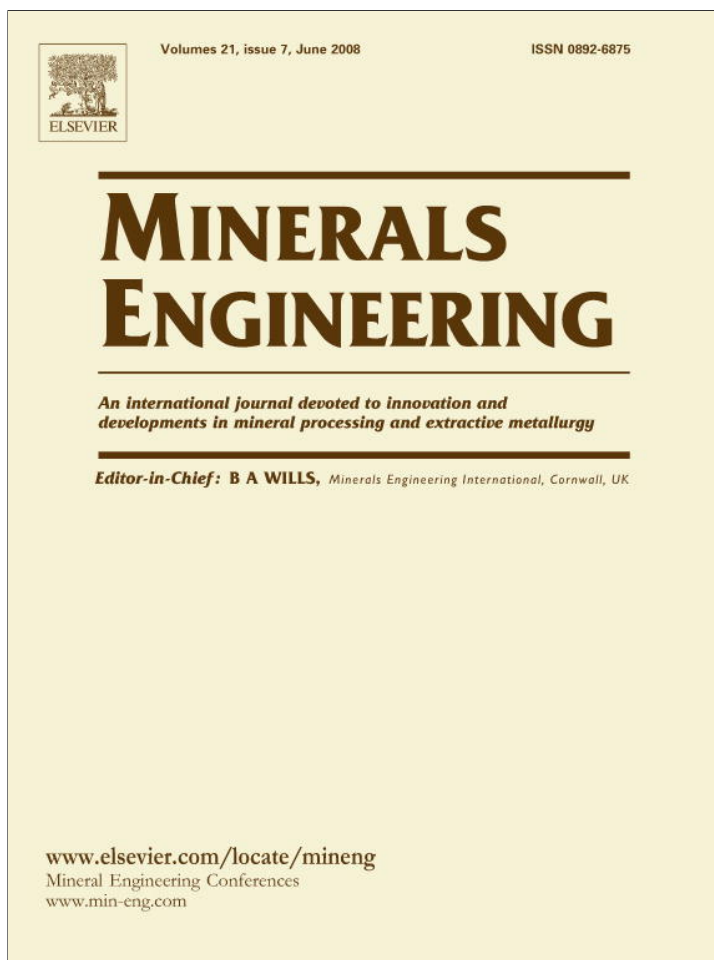


Provided for non-commercial research and education use.
Not for reproduction, distribution or commercial use.



This article appeared in a journal published by Elsevier. The attached copy is furnished to the author for internal non-commercial research and education use, including for instruction at the authors institution and sharing with colleagues.

Other uses, including reproduction and distribution, or selling or licensing copies, or posting to personal, institutional or third party websites are prohibited.

In most cases authors are permitted to post their version of the article (e.g. in Word or Tex form) to their personal website or institutional repository. Authors requiring further information regarding Elsevier's archiving and manuscript policies are encouraged to visit:

<http://www.elsevier.com/copyright>



Techniques and applications for predictive metallurgy and ore characterization using optical image analysis

G.R. Lane^{a,*}, C. Martin^b, E. Pirard^c

^a *Rio Tinto Technology and Innovation, 1 Research Avenue, Bundoora, Victoria 3083, Australia*

^b *SGS Mineral Services, Kent Corporate Centre, Vancouver, British Columbia, Canada*

^c *University of Liege, 4000 Liege, Belgium*

Received 28 October 2007; accepted 21 November 2007

Available online 14 January 2008

Abstract

Optical image analysis (OIA) as a predictive metallurgical tool has been advanced by work completed at SGS Mineral Services by integrating a standard image analysis system with innovative preparation methods and measurement techniques. The preparation of sized material into non-touching particle polished sections as well as the selective coating of epoxy facilitates the recognition of non-opaque minerals, thus correctly identifying locked and complex particles. Advanced data analysis enables the preparation of predictive metallurgical data. Test cases were compared to metallurgical test results including size distribution, mineral release and grade/recovery data for various ore deposits. The limiting factor in direct optical image analysis is the discrimination between minerals with similar reflective properties. Advances made at the University of Liege have made it possible to optically distinguish these minerals using multispectral imaging. Integrating these technologies will enable OIA to be an affordable and viable alternative for gathering process mineralogical data.

© 2007 Elsevier Ltd. All rights reserved.

Keywords: Ore mineralogy; Liberation; Liberation analysis

1. Background

The basics of microscopy have been applied to mineral identification for over a 100 years beginning with the study of metals and meteorites by Sorby in 1861. The first microscopes were poorly illuminated and often relied on chemical etching to assist in distinction between minerals. In the early 20th century Murdoch (1916) detailed the colour and reflectance of ore minerals and used micro-chemical techniques to identify minerals. His work was later expanded by other mineralogists to include photometric measurements, and polarizing techniques. As microscopes and optical lenses improved over time other properties of minerals were observed. In 1962 the Commission on Ore Micro-

scopy produced a Table of Quantitative Data which contained the incorporation of reflectance standards to assist in mineral identification. The table included, for the first time, the reflectance data of minerals for four wavelengths (470, 546, 589, and 650 nm) and was eventually published as the quantitative data file (QDF) (Criddle, 1998). The work of mineralogists such as Ramdohr (1969), Uytendogaardt and Burke (1971), Craig and Vaughan (1981), Picot and Johan (1982) have presented this data along with detailed descriptions for use by mineralogists to identify the ore minerals. Currently OIA systems purchased “off the shelf” are often developed for metallography or the biomedical industries and include no mineralogical recognition database software. Recognition is dependant upon the ability of the user. In the future advanced OIA systems for mineralogical applications would employ the use of this QDF database and specific wavelength filters for automated mineral identification. It must be remembered that

* Corresponding author. Tel.: +61 3 92423326; fax: +61 3 92423222.
E-mail address: geoff.lane@riotinto.com (G.R. Lane).

these “off the shelf” systems are still of value to the mineralogist and have been utilized effectively to carry out quantitative mineral analysis on simple ore types.

2. Imaging

In the past digital imaging has had limited quantitative use and has been restricted to the presentation of photomicrographs detailing relative textures that influence recovery and/or grade. In order to more effectively apply current technology to quantitative mineral analysis it is important to understand how the digital imaging equipment gathers this information, since the image acquisition has the greatest effect on the performance of any imaging system. In plane incident light the accurate representation of the reflectance spectrum of the mineral components is essential to reduce misidentification and accurately quantify mineral proportions and other attributes.

Digital cameras used in optical microscopy usually incorporate a charged-coupled device (CCD) to capture images. The CCD transfers the optical photon data received through a filter into electronic pulses or photogenerated electrons. Voltage created is then converted to pixels using an analog to digital converter (ADC) and stored until the entire number of pixels representing the image are captured and then presented in their entirety on the monitor for visual inspection (Spring et al., 2007). Three methods for compiling a colour image using a CCD digital camera exist as follows:

1. Three chip CCD
2. Bayer mosaic filter
3. Three shot colour sampling

The three chip CCD is primarily used on analog cameras, where each chip is located under the lens and collects images representing the red, green and blue regions of the spectrum (Fig. 2). These are then merged to form a single image using compiling hardware and software. A Bayer mosaic filter is a single filter having alternating pixel areas of red, green and blue in front of an imaging sensor. Software and hardware are employed to interpolate between the varying pixels to form a single colour image. This adequately represents colour as viewed by the human eye and is primarily centered around the 450, 550, and 650 nm ranges for blue, green and red, respectively (Fig. 1, Pirard, 2004). Finally a three shot colour sampling system employs the collection of three separate images of the entire CCD using filters representing red, green, and blue regions of the spectrum (Kuyatt et al., 2007). These three images are then merged to make a single colour representation of the item. This is based upon a mobile RGB filter or LCD (liquid crystal display) filter that changes colour in response to an applied voltage.

OIA systems designed for metallography, can be applied to mineralogy after some modifications to allow for specific data requirements. The basic criteria for an optical image

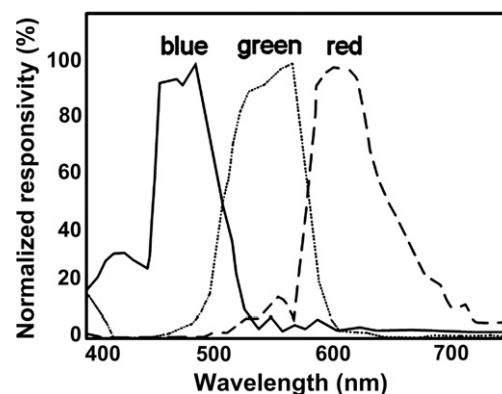


Fig. 1. Typical RGB filter transmittance curves used in digital colour imaging (Pirard, 2004).

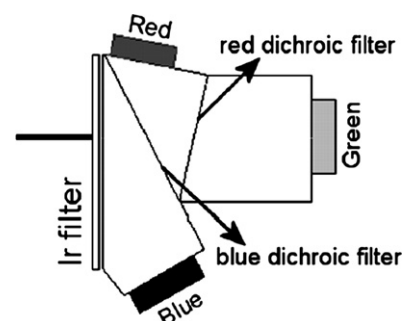


Fig. 2. 3 CCD sensor fitted to a prism to discharge specific colour electrons (Pirard, 2004).

analysis system include an incident light microscope (reflected light), automated stage controlled by an integrated imaging software package and a digital camera. The equipment used at SGS minerals included a 3 CCD Sony analog camera attached to a Nikon ME600 microscope, Clemex Vision PE software and automated stage. In order to correctly analyze the mineral specimens some hurdles must be crossed that have made the quantitative analysis of minerals from polished sections a difficult task for optical systems. These include:

- Density settling of heavy minerals and coarse particles.
- Touching particles.
- Discrimination of non-opaque gangue minerals from the epoxy.
- Reflectance overlap of minerals.

3. Sample preparation

SEM-based technologies were developed to overcome some of these difficulties and include methods such as graphite inclusion. The addition of graphite to the epoxy helps reduce some of the density settling of the minerals as well as remove/reduce particle touching, but this is not practical for optical systems because the reflectance and

colour of the graphite can overlap with mineral species. An alternative proprietary method was used that allowed for the removal of density segregation as well as limit particle touching. Fig. 3 presents two images of polished sections prepared from the same sample using the standard preparation method (A) and the non-touching method (B). The removal of touching particles allowed for the accurate determination of chalcopyrite liberation where image A illustrates the congested surface which yielded a measured result of 60% liberation of chalcopyrite due to the high packing density and the touching of particles. In contrast, image B illustrates a much lower packing density and significantly improved liberation result for chalcopyrite (~90%). The example in this case was a very fine fraction ($-20 + 10 \mu\text{m}$) that contained some closely packed particles that can be treated using standard image analysis techniques. Coarser fractions yield a better separation of particles.

For many years the distinction between non-opaque minerals and the epoxy has been an issue when applying the technology to metallurgical feed samples. Considerable evaluation of many types of epoxies or fillers has been undertaken to try and create a distinction between these low reflective minerals and epoxy that exhibit similar colours and reflectivities when observed using plane incident light. The sensitivity and dynamic range of many digital cameras has improved to the point that distinction can now be made between certain more reflective non-opaque minerals and epoxy. These minerals include apatite, amphibole, calcite, and garnets, although quartz still remains the most difficult. In order to apply OIA to the field of process mineralogy it was imperative to be able to determine the opaque ore mineral association with all non-opaque gangue minerals in feed, concentrate, or tailing samples. In many cases the actual identification of the non-opaque minerals can be completed using other techniques such as X-ray diffraction. It is the overall group of non-opaque mineral association with particular ore minerals that often provide the most critical information.

A simple solution has been employed that allows a coating to be applied to the epoxy, but nevertheless retains the

natural optical properties of the minerals using a carbon coater. Samples were coated with carbon at slightly extended times to allow a dark coating of carbon (~45 nm) on the surface of the polished section. This was done at one time as multiple coatings resulted in different coloured layers of carbon that would flake off at varying rates. The coated section was lightly polished using water and light pressure on a DAC polishing cloth (Struers) for less than a minute. This was repeated until the mineral surfaces were exposed, leaving the epoxy covered. Preferential adhesion of carbon to the epoxy relative to the mineral surfaces as well as differences in relief permits a gentle polish to remove carbon from mineral surfaces. Difficulties arose primarily with porous minerals (e.g. Fe oxy-hydroxides) where deposited carbon in micro-pore spaces is difficult to remove. Application of this technique for primary base metal sulphide and iron ore minerals has proved successful. Fig. 4 illustrates a coated polished section where the exposed mineral surface is free of carbon and the epoxy remains coated. The colour variation between the hematite exsolution lamellae and the coated epoxy is sufficient enough for the OIA to make the distinction.

4. Software

The Clemex Vision PE software allows for the mineralogist to create the analysis macros suited to the minerals present and the information required. This may entail gold search routines, liberation and association routines, porosity and physical property (aspect ratio) or compilations of these parameters into a single routine. The main application discussed here will be the use of a routine compiled to determine the mineral associations and ore mineral liberation.

Initially the minerals are identified by the mineralogist and assigned into categories identified as bitplanes. The thresholding of these bitplanes involves the reflectance intensity of the mineral and the reflectance spectrum generated using the RGB camera. Often in simple mineral suites the differences in the opaque mineral are great enough to make a clear distinction using these two parameters. As

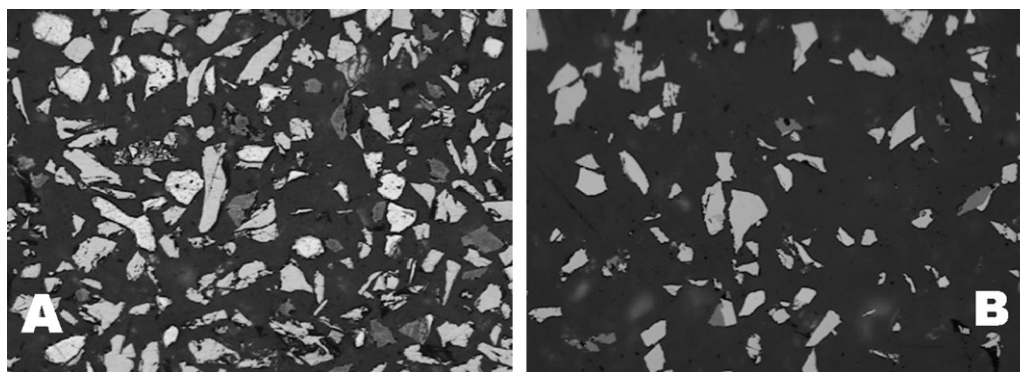


Fig. 3. A Cu concentrate $-20 + 10 \mu\text{m}$ fraction prepared by two separate methods. Image A was taken of a polished section prepared using standard techniques, yielding a measured ~60% liberation of chalcopyrite. Image B taken from a polished section of the same sample prepared using non-touching techniques and resulting in a 90% measured value for liberation of the chalcopyrite.

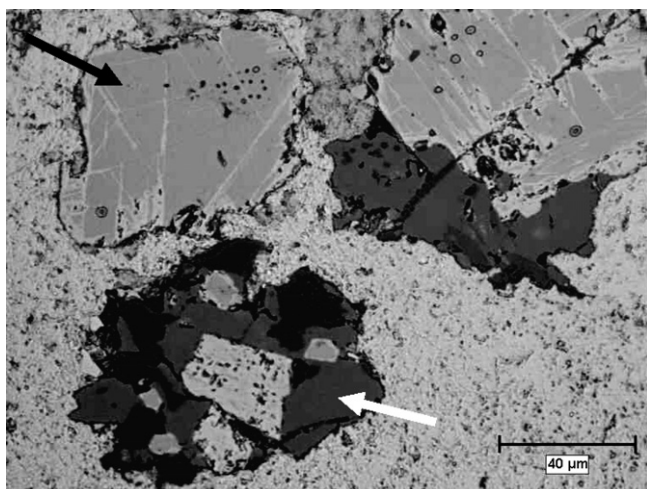


Fig. 4. A +200 mesh size fraction of an Iron Ore feed sample illustrating the surface of the particles and epoxy after partial carbon removal. The epoxy remains coated with a thick layer of brownish carbon. The photomicrograph shows magnetite grains as liberated particle (black arrow) and as attachments and inclusions in non-opaque mineral (white arrow). Fine hematite exsolution lamellae are evident in the larger magnetite grains.

an example the reflectance intensity and spectra for chalcocopyrite and pyrite are easily distinguished using these parameters because the pyrite has a slightly higher reflectivity and the chalcocopyrite a more prominent reflectance spectrum towards the green wavelengths. At times some of these parameters are similar or may have a slight overlap due to polishing effects or compositional alteration. Image analysis tools such as chord sizing, erosions, and boolean logic are employed to ensure representation of the mineralogical attributes. If pixel overlap occurs boolean logic statements were included to remove foreign pixels before measurements were taken, because this would result in the same area being counted twice. Area and grain size measurements are carried out on the identified bitplanes. A sequence of coloured images is presented in Fig. 5 illustrating the consecutive assignment of the mineral components as bitplanes from the captured image. The relative data are measured and the image is discarded to reduce memory size, but the location of the data is stored and the image outline is retained for relocation. The measured data includes the particle area along with the composite grain area. Additional features such as aspect ratio, grain exposure, and porosity can also be measured and used to group mineral properties. Other work has been carried out which measured these additional properties for process mineralogical characterization of feed material, but the primary objective of the initial phase of development was to determine the mineral abundance and mineral associations that result in overall liberation.

Since the variety of mineral combinations in a single feed sample can be large, it became apparent that not all the possible combinations and mineral liberation categories could be presented the Clemex software. An Excel macro was therefore created to carry out the rigorous calcula-

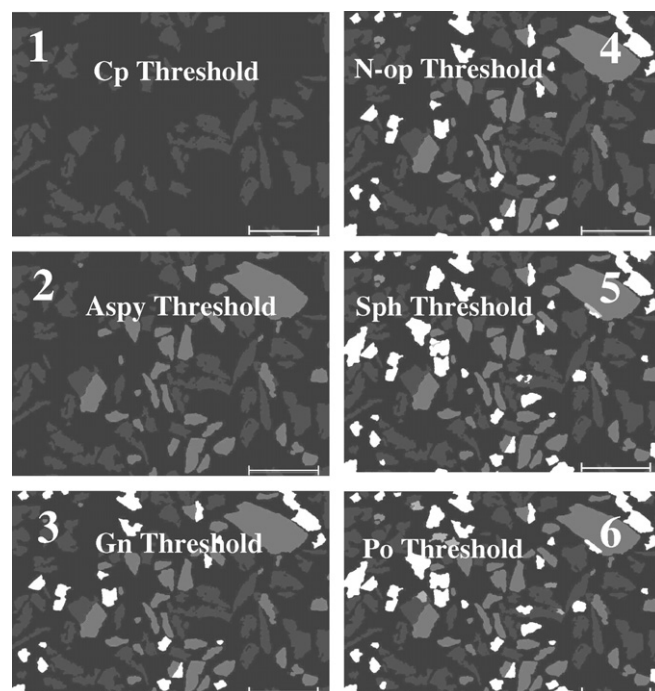


Fig. 5. Consecutive imaging of a single field where each mineral component is given a colour bitplane based upon the colour and intensity.

tions involved to determine mineral abundance, mineral association, and liberation categories based upon basic data obtained using the Clemex software. The Clemex system was then used as a tool to capture raw data and autopopulate a basic spreadsheet for further characterization using Excel. This resulted in increased speed of data acquisition and a greater flexibility in data calculations. On average, a complex mineral assemblage of 8 minerals requires approximately 20–30 min to gather data for in excess of 20,000 particles using the OIA system. Once the data was gathered it was inserted into the Excel macro to carry out the data categorization, and sum the overall mineral abundance, amount of liberated particles, and detailed mineral associations in approximately 5 min. Individual particle data detailing the area of the total particle, as well as the areas of the grains that comprise the particle, are inserted into the macro and processed. The maximum number of permissible entries in Excel is 65,000 limiting the number of particles that can be measured in one polished section. The image analysis system can collect data for more than 300,000 particles, but the 65,000 particles per size fraction limit in Excel still provides a statistically viable quantity of particles. In comparison the number of particles usually measured using particle mapping analysis in SEM-based technologies is usually under 5000 per size fraction.

The macro sorts and calculates the raw data to provide:

1. Mineral proportions.
2. A summation of the mineral associations sorted into 10% liberation categories.

Area μm	FeretAvg μm	Cp μm	Py μm	Ox μm	NOG μm	Cov μm	St μm	Bn μm	Dig μm
35635	239	8819	24994	0	1822	0	0	0	0
26903	227	5537	0	0	21366	0	0	0	0
16082	168	2297	0	0	13785	0	0	0	0
49917.2	352.833	1945.04	5403.62	0	42568.5	0	0	0	0
1823	66	1566	0	0	0	259	0	0	0
93207	478	1451	0	0	91756	0	0	0	0
25288.8	247.468	1174.27	0	0	24114.5	0	0	0	0
32293	230	1033	0	0	31261	0	0	0	0
32690	238	972	0	0	31718	0	0	0	0
5544	144	591	0	0	4952	0	0	0	0
45356.8	281.535	505.611	0	0	44851.2	0	0	0	0
58048	334	492	0	0	57556	0	0	0	0
18155.9	171.478	378.797	0	0	17777.1	0	0	0	0
15371	228	331	0	0	15040	0	0	0	0
45373	305	303	0	0	45070	0	0	0	0
1885.75	65.4439	296.45	0	0	1589.3	0	0	0	0
12831	150	295	0	0	12537	0	0	0	0
105823	439.601	271.746	0	0	105551	0	0	0	0
70420	404.128	237.16	0	0	70182.8	0	0	0	0
14235	166	237	0	0	13997	0	0	0	0
31228	279	234	0	0	30994	0	0	0	0
60029	359	161	0	0	59888	0	0	0	0
1355.43	64.5517	0	0	0	0	0	0	1355.43	0
88135	378	0	0	0	87733	0	0	446	0

Fig. 6. Selected image of raw data exported into the Excel macro. Mineral abbreviations include Cp – chalcopyrite, Py – pyrite, Ox – oxide, NOG – non-opaque gangue minerals, Cov – covellite, St – stannite, Bn – bornite, Dig – digenite.

3. Frequency of particles and grain size data.
4. Cumulative mineral grade data by weighting liberation as a measure of recovery potential in order to determine theoretical mineralogically controlled grade and recovery data.

Further calculations such as mineral release curves, mineralogically limiting metal grade and recovery can be performed using this base data from the macro. This resulting data are considerably more compatible with process mineralogical requirements than standard reports generated from the Clemex program. Fig. 6 presents a snapshot of a portion of the raw data that is inserted into the OIA macro.

5. Case study – Cu, Pb, Zn process mineralogy

OIA has been effectively used for process mineralogical evaluation of feed samples to assist in the characterization of the samples prior to flotation testwork. Samples are often ground to ~85% passing 150 μm and screened into four size fractions depending upon the sample. The average metal grade dictates the number of polished sections prepared from each size fraction. The following case study of data obtained from a Cu, Pb, Zn, volcanogenic massive sulphide (VMS) deposit illustrates how the OIA system has

been employed for characterization of feed material before froth flotation.

The sample was ground to 85% passing 75 μm and screened at 150, 75, 38, 20 and 10 μm each being submitted for chemical assay and the preparation of polished sections. Each of the polished sections was analyzed using the OIA system applying an appropriate magnification for each size fraction. Through the acquisition of the data by OIA and the sorting of the data through the Excel macro, modal mineral distributions (Fig. 7) and mineral associations for each size fraction (Fig. 8) are produced. The mineral abundance was qualified by balancing the stoichiometric metal content against assay values for each size fraction. The mineral abundance in weight% is not stereologically corrected because the increased particle frequency, more random nature of the particle orientation from the non-touching particle sectioning method, and the sizing of the material into six size fractions assists in reducing the effect of stereology on the results.

The image analysis data can graphically present textural information that influences grade/recovery and liberation for metallurgical scoping. The texture of the material examined was such that galena was finely intergrown with sphalerite and pyrite making it difficult to achieve full liberation. The photomicrographs in Figs. 9 and 10 illustrate the textures observed within these size fractions. The portrayal of these textures as graphical data is illustrated in the grade recovery curves for zinc and lead. The mineralogically determined grade/recovery for zinc (Fig. 11) illustrates an upgrade potential consistent with a coarse grain size which is easily liberated and amenable to flotation. The mineralogically determined grade/recovery curve for lead (Fig. 12) indicates that the material is more difficult to liberate and yields more attached grains and binary particles at the current grind size, thereby limiting recovery and diluting the grade. Similarly, this is demonstrated in the release curves for sphalerite, chalcopyrite and galena in Fig. 13. The graph illustrates the percentage liberation in successive fractions attained for the grind. Using the inflection point of the mineral liberation curve, the graph can illustrate the particle size at which effective and/or maximum liberation is achieved, and thus the coarsest size at which effective recovery becomes viable. These sizes are governed by the minerals natural grain size for “release” or liberation, and points to the optimum primary and regrind sizes. The curves for both chalcopyrite and sphalerite in Fig. 13 demonstrate that these minerals would achieve maximum liberation (~90%) between 15 and 25 μm, an

Mesh	Microns μm	Cp	Py	Gal	NOG	Sph	Enargite	Total
+100	150	1.7	26.7	0.3	66.0	5.2	0.1	100
+200	75	1.5	54.9	0.6	25.0	18.1	0.0	100
+400	38	0.8	62.8	4.1	14.4	17.9	0.0	100
+635	20	1.3	64.7	1.8	14.5	17.7	0.0	100
-635	10	2.2	58.2	2.6	14.7	21.4	0.9	100
	-10	2.4	48.3	2.2	23.4	22.6	1.1	100

Fig. 7. Modal abundance as weight% for each size fraction and includes the –10 μm fraction as measured by OIA. This data has no stereological correction and uses theoretical mineral density values.

Size Range	+150µm						+75µm					
	Cp	Sph	Gal	Py	NOG	En	Cp	Sph	Gal	Py	NOG	En
Liberated	29.9	42.9	19.0	25.2	80.5	12.3	33.6	47.1	4.2	52.2	83.1	46.6
Binary -Cp	---	4.5	20.5	19.6	13.0	8.6	---	3.9	0.1	10.4	2.7	12.9
Binary -Sph	2.9	---	1.9	6.7	0.8	0.4	13.6	---	0.1	16.0	0.0	3.0
Binary -Gal	0.0	0.7	---	2.6	0.0	9.0	0.0	0.2	---	5.7	0.0	0.0
Binary -Py	19.8	17.2	20.6	---	0.5	5.9	23.3	21.7	55.2	---	2.5	3.0
Binary -NOG	12.4	5.0	0.0	0.8	---	0.6	1.5	6.4	0.0	1.3	---	0.0
Binary -En	1.3	0.0	0.0	1.3	0.0	---	1.1	0.0	0.0	0.0	0.0	---
Ternary	21.5	19.0	27.2	41.2	4.5	44.7	23.8	16.7	32.4	12.2	10.3	10.0
Complex	12.1	10.9	10.9	15.5	0.8	18.7	3.1	3.9	8.0	2.1	1.4	24.5
Total	99.9	100.1	100.0									
Modal Abundance Wt., %	1.7	5.2	0.3	26.7	66.0	0.1	1.5	18.1	0.6	54.9	25.0	0.4

Fig. 8. Mineral associations as weight% for the +150 and +75 µm size fractions measured by OIA and sorted and calculated using an Excel macro.

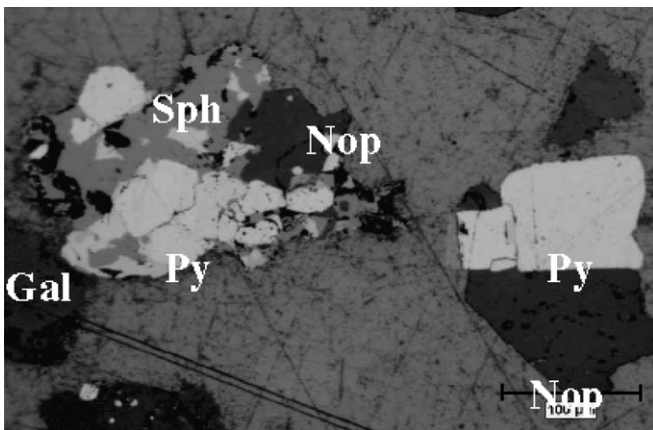


Fig. 9. A composite particle containing sphalerite, pyrite, galena and a non-opaque mineral (left) illustrating the tightly intergrown texture that may affect liberation and flotation.

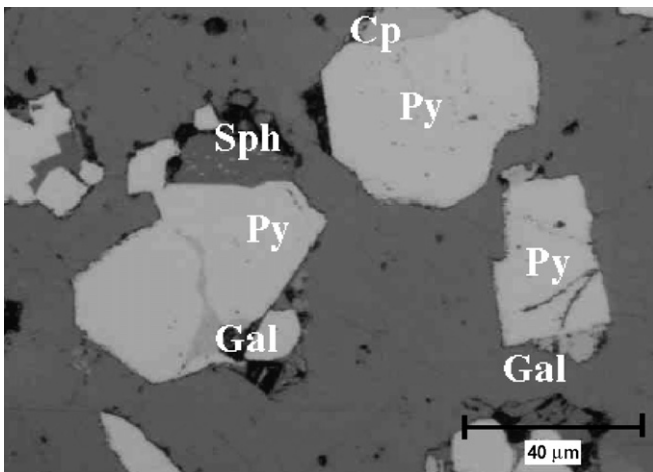


Fig. 10. Ternary particle of pyrite, sphalerite and galena (left) and two particles showing simple binary association of pyrite and chalcocopyrite (top) and pyrite and galena (right).

indication of the target regrind size for those minerals. (A liberated particle is this study was determined to be >80% of the mineral of interest.) Galena in this graph illustrates no inflection; suggesting a linear release of the mineral results in having to regrind to a very fine size (<10 µm) to achieve maximum liberation.

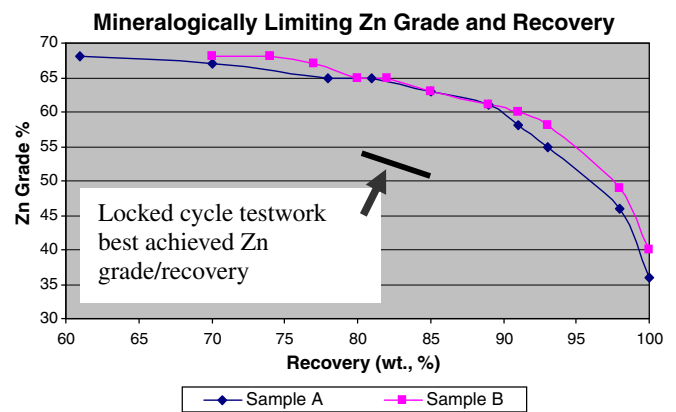


Fig. 11. Mineralogically determined Zn grade vs. recovery from VMS deposit. The achieved Zn grade/recovery from locked cycle testwork is also indicated.

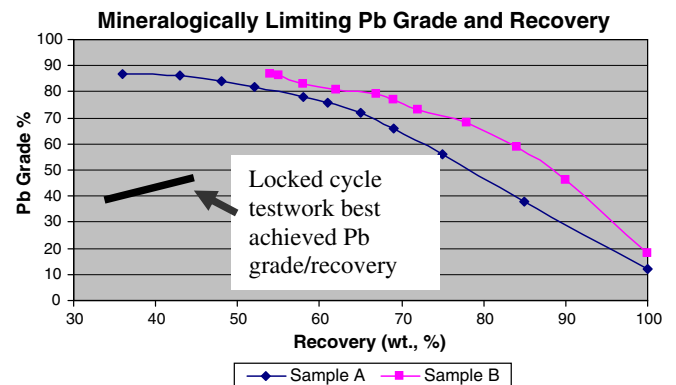


Fig. 12. Mineralogically determined Pb grade vs. recovery from VMS deposit. An indication of the textural relationship of the Pb bearing minerals suggests a much poorer grade/recovery for Pb. This was also demonstrated in the results from locked cycle testwork as indicated.

The grade recovery curves determined mineralogically outline the theoretical grade and recovery based upon only the mineral components and the relationship to gangue. Seldom has it been demonstrated that separation test work can achieve this theoretical result. Usually the best separation can be within 10% of the mineralogical limit established by OIA. In this case the locked cycle test work for these samples supports the findings that were determined by OIA of the sized feed material. The grade/recovery of

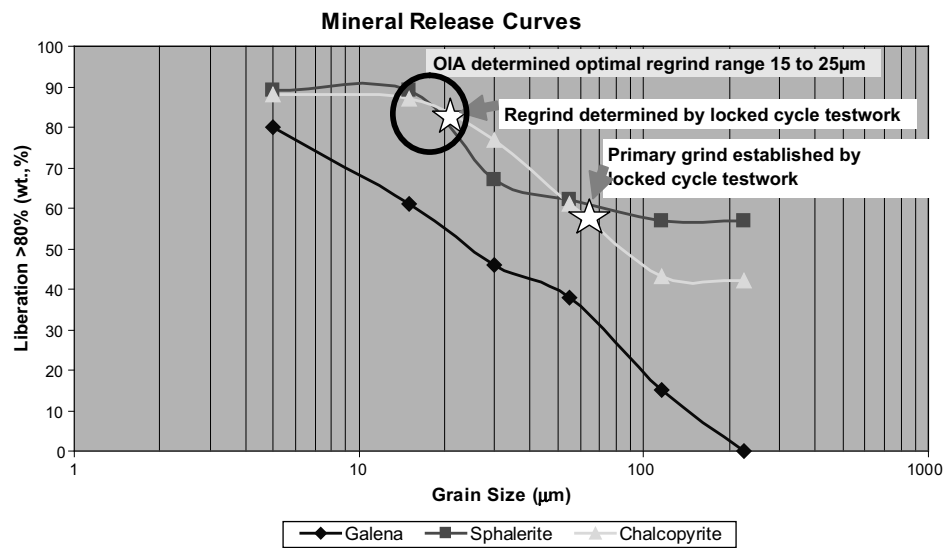


Fig. 13. Liberation by size curve demonstrating the potential regrind size for chalcopyrite and sphalerite at the inflection point of the curve between 15 and 25 µm as indicated by the black circle. Galena shows a linear relationship between size and liberation indicating poorer Pb performance. The locked cycle testwork established a primary grind of the ore at approximately 70 µm and a further regrind at 22 µm, within the range indicated by OIA.

Zn by flotation paralleled the theoretical values established by OIA. The Pb grade/recovery curves from metallurgical test work indicated a much poorer result where Pb achieved at best 42% Pb and 47% recovery. This is a reflection of the poorer Cu/Pb selectivity common in these ore types during flotation test work. The resulting metallurgical curve for Pb does not follow the theoretical mineralogically limiting curve due likely to the variation in flotation chemistry (selectivity) and is not a reflection of the liberation characteristics of the ore. Often the plant performance will exceed those achieved by the locked cycle test work due in part to the better froth drainage and tighter particle size distribution from the primary and regrinding circuits.

This case study demonstrates the power of the data obtained using an OIA system for relatively straight forward or simple mineral assemblages. The benefits of this type of system include its speed of gathering data, simplicity of functional equipment and relatively low cost. The resulting data are often inter-changeable with SEM-based systems. Indeed the substantial database now gathered by SGS using both QemSCAN and OIA systems show the data, in terms of their ability to predict metallurgical flow-sheet performance, on simple ores, are fully inter-changeable (unlike optical point-counting methodologies, which exhibit significant bias especially in terms of liberation and predicted primary and regrind sizes). The limiting factor of using OIA is often the complexity of mineral content and non-opaque gangue mineral resolution. In most applications to mineral processing the identification of the non-opaque mineral species in detailed liberation is unnecessary and can be grouped together as non-opaque minerals and then characterised by qualitative or quantitative powder X-ray diffraction. The difficulty remains when opaque minerals illustrate similar colours and reflectivities in plane light making it virtually impossible to distinguish them

apart using standard digital imagery and software. An example of some of the more common overlapping minerals includes pentlandite, and violarite, covellite and chalcocite, or cubanite and pyrrhotite. These minerals (and others not listed) are difficult to distinguish by automated means, whereas the mineralogist often relies on other properties such as birefractance or anisotropy to make a positive identification. This overlap in spectral signal of minerals has led to the more common use of scanning electron microscopy (SEM) to distinguish mineral species using energy dispersive X-ray spectrometry (EDX) or backscatter brightness in automated mineralogy. The drawbacks of SEM-based systems are often the high capital and operating costs, and the dust-free, climate controlled environment in which they must operate. These constraints leave room for a more robust, cheaper and easily maintained system that can provide the data with sufficient statistics and accuracy for predictive metallurgical applications such as mineralogical-based on-site production forecasting or geometallurgical mapping, where speed, simplicity and cost rank as important as data precision. With the deficiencies in OIA considered and in order to perform well with all mineral combinations, OIA systems will need to employ a method of removing spectral overlaps existing between minerals in more complex assemblages. Once this is fully employed this will provide a far cheaper alternative to SEM-based systems.

6. Multispectral Imaging

The inclusion of wavelength responses within the QDF (quantitative data file) gives a basis for the development of multispectral systems that use specific wavelengths to distinguish mineral species that exhibit overlapping spectral responses. The use of advanced computer and microscopic

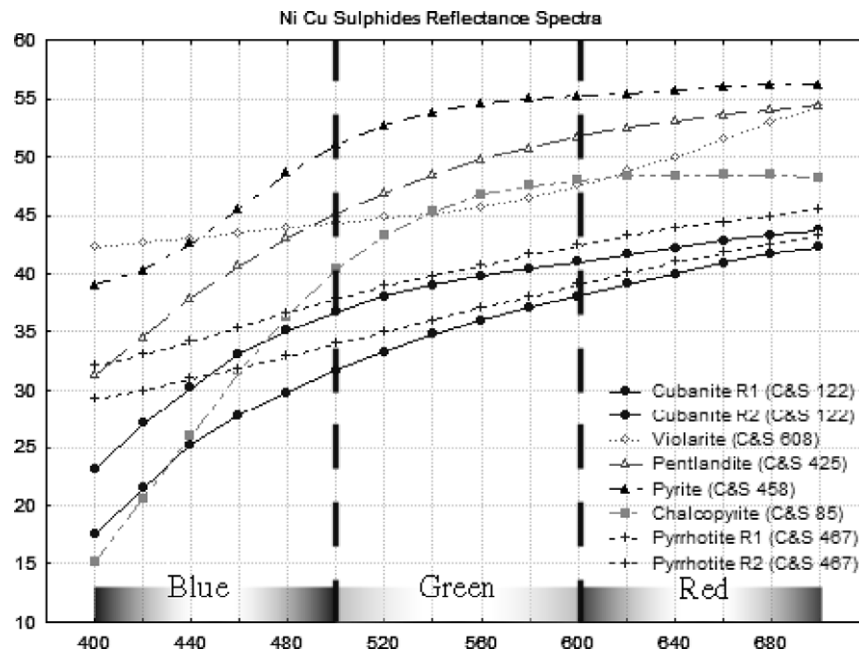


Fig. 14. Reflectance intensity across the wavelength spectrum for six different minerals. The three panels indicate the wavelength groupings used in RGB colour imaging.

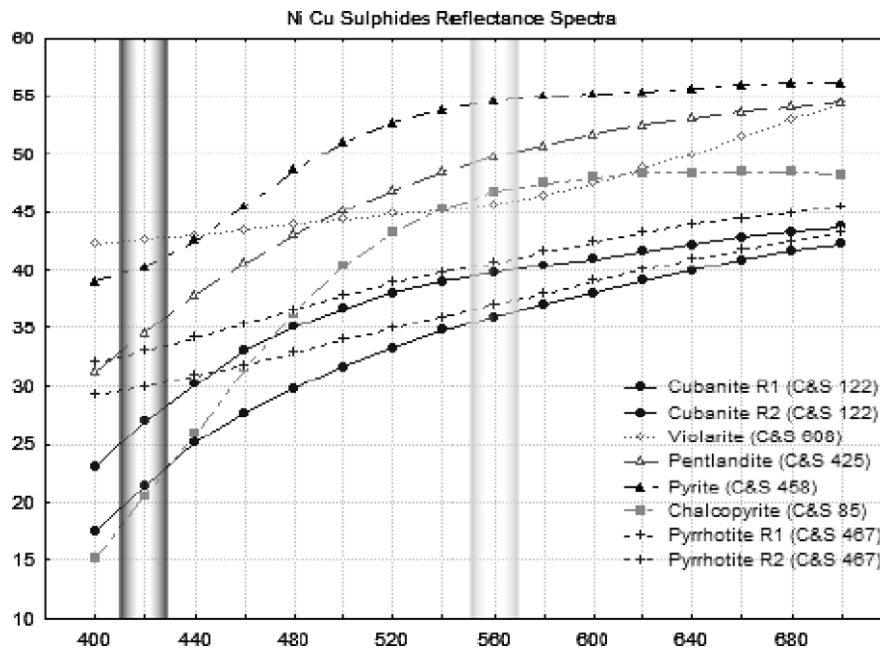


Fig. 15. Reflectance intensity across the wavelength spectrum for six minerals, illustrating specific filter “channels”.

integration now provides the tools necessary to take advantage of information gathered over the past 30 years. The development of reflectance standards and reflectance properties was last published by Criddle and Stanley in 1993 updating work first begun by Henry in 1977. With this data and the use of filter wheels, which are common attachments to compound microscopes in the biomedical field, a system can be constructed that allows for the phase segmentation of minerals that exhibit similar spectral signals in plane

RGB light. A filter wheel equipped with a number of narrow bandwidth interference filters inserts the selected filter into the light path of the incident light to constrain the wavelengths of light that cause the overlap between minerals.

The response of minerals under the full visible light spectrum is grouped into three packages for colour cameras (RGB) as discussed previously. Fig. 14 illustrates the spectral signatures for a series of common Ni, Cu sulphide

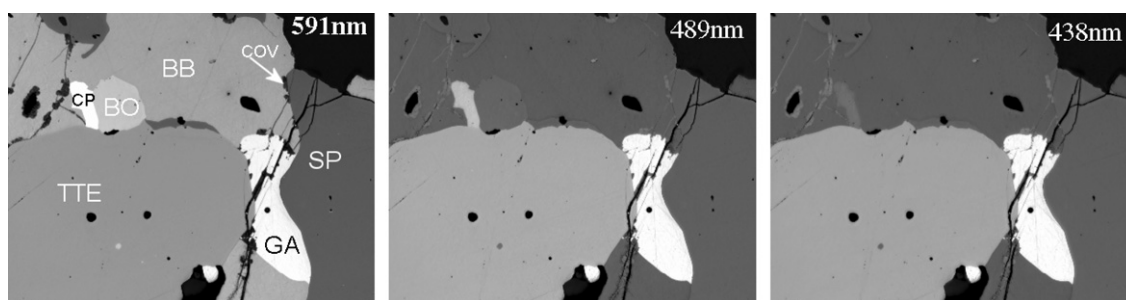


Fig. 16. A single field of view taken at the wavelengths of 591, 489, and 438 nm illustrating the reflectance variation of the mineral constituents. Chalcopyrite (Cp); Orange Bornite (BO); Brown Bornite (BB); Tetraedrite (TTE); Sphalerite (SP) and Covellite (COV).

minerals that often cause problems with standard image analysis systems. The three panes labeled red, green, blue, indicate how the RGB signal groups these wavelengths together to represent a colour image. This results in the overlap of spectral signals making it difficult for an OIA system to separate some mineral species. In this example one can see the close similarity in spectral response for cubanite and pyrrhotite, as well as chalcopyrite and violarite. If a wavelength specific filter is used, a specific “channel” can be used to separate out the mineral overlaps, in this case Fig. 15 illustrates the resolution to be achieved by the insertion of a 420 nm filter to separate cubanite from pyrrhotite and chalcopyrite from violarite and a second filter image at 560 nm to separate chalcopyrite from cubanite. The typical interference filters used for spectral segmentation include 360, 438, 489, 546, 591, and 692 nm. Using the Clemex software it is possible to image the same field at a number of different wavelengths saving each image and then overlaying the images to resolve each of the mineral overlaps. This synchronized image capture provides an advantage to discriminating between similar phases. Fig. 16 illustrates progressive photomicrographs of the same field are taken at 591, 489, and 438 nm illustrating the significant variation of reflectance between minerals with similar spectral reflectance.

The addition of multispectral imaging to standard OIA systems like those employed at SGS Minerals creates many possibilities for a simple and cost effective means to carry out process mineralogical ore characterization. The optical distinction between minerals using specific wavelengths significantly reduces the number of minerals that have overlapping optical signatures making OIA a technique that can be applied to many ore types. This advance in optical microscopy allows for the potential for a revolution of process mineralogical examination making it possible to put lower cost, more robust analysis systems into remote and difficult localities or small processing facilities where more costly and complicated SEM units would be impractical.

7. Conclusions

The use of optical microscopy for mineral identification has been a standard in the mineral industry for

many years. The development of more powerful imaging and computing tools now allows for the full automation of the optical microscope to carry out quantitative mineralogical analysis. The application of these tools for process mineralogical characterization of feed material for flotation has been successfully applied demonstrating the potential for growth in this area in the mining sector. Potentially, “off the shelf” image analysis systems can be used for the application of this basic technology and the application of multispectral imaging. The use of integrated microscopes with image analysis software allows for routines to be constructed that enable multi-image grabbing of the same field along with the overlapping of these images to distinguish between phases, as well as the control of the filter wheel that allows specific filters to be inserted at specific times within the routine. This control of the microscope, and data acquisition allows for a much more powerful tool for the mineralogist. It is the goal of multispectral imaging that an auto recognition system be put in place using the QDF information database that will allow for automatic identification of the ore minerals using an optical microscope. A tool of this nature would provide a much more robust method to be deployed at remote mine sites or low cost operations that could benefit from automatic quantitative mineral analysis. The integration of this type of recognition equipment with the data sorting and process mineralogical data analysis will provide a valuable tool for the mineral processing industry in the future.

References

- Craig, J.R., Vaughan, D.J., 1981. *Ore Microscopy and Ore Petrography*. John Wiley & Sons, NY, p. 406.
- Criddle, Stanely, 1993. *Quantitative Data File for Ore Minerals*, third ed. Chapman & Hall, London UK, p. 635.
- Criddle, A.J., 1998. Ore microscopy – photometry. In: Cabri, L.J., Vaughan, D.J. (Eds.), *Modern Approaches to Ore & Environmental Mineralogy*, Commission on Ore Mineralogy. International Mineralogical Association, pp. 10–67.
- Henry, N.F.M. (Ed.), 1977. *IMA/COM Quantitative Data File*, first issue. International Mineralogical Association – Commission on Ore Microscopy. McCrone Research Associates Ltd., London, England.
- Kuyatt, B.L., Weaver, R., Merlo, P., 2007. *Image Capture Methods*, <www.diaginc.com/techforum/AdvanMaterlsArticle.pdf>.

- Murdoch, J., 1916. *Microscopical Determination of the Opaque Minerals*. John Wiley & Sons, NY, p. 165.
- Picot, P., Johan, Z., 1982. *Atlas of Ore Minerals*. BRGM/Elsevier, Orleans, France/Amsterdam, The Netherlands, p. 458.
- Pirard, E., 2004. Microspectral imaging of ore minerals in optical microscopy. *Mineralogical Magazine* 68 (2), 323–333.
- Ramdohr, P., 1969. *The Ore Minerals and their Intergrowths*, second ed. Pergamon, Oxford, UK, p. 1205.
- Spring, K.R., Fellers, T.J., Davidson, M.W., 2007. Digital Imaging in Optical Microscopy, Nikon MicroscopyU: Fundamentals of Digital Imaging. <www.microscopyu.com/articles/digitalimaging/ccdintro.html>, p. 19.
- Uytenbogaardt, W., Burke, E.A.J., 1971. *Tables for Microscopic Identification of Ore Minerals*. Elsevier, Amsterdam, The Netherlands, p. 430.